# Optimisation of a fishing kayak.

Alfred Thompson
Subsystem 1: Hull optimisation

Gabriele D'Amone
Subsystem 2: Paddle Optimisation

Ruksana Shaukat Jali
Subsystem 3: Motor optimisation

Melisa Mukovic
Subsystem 4:

***Abstract*- The following report is the documentation of the optimisation for speed of a fishing kayak which can be either human-powered with the use of a paddle or propelled by a motor. The problem was split into four subsystems – hull design, paddle design, trolling motor and seat position. This allowed for a more in-depth analysis of different factors affecting the final output. The outcome of the first subsystem was the optimization of the kayak hull for a 8.9% increase in performance. Through the second subsystem an output average thrust of 58.8 N was received as the optimal value. The third subsystem found the maximum motor thrust obtainable to be 1820 N. The fourth subsystem took into consideration the relationship between seat height and paddling efficiency, as well as boat stability – the output was the optimal position of center of gravity equal to 0.14 m above waterline. Overall, on the system level the final speed of a fishing kayak was 3.0 m/s for human-powered and 10.0 m/s for motor-powered scenarios.**

***Keywords— Optimisation, Kayak, Motor, Hull, Paddle, Seat***

## I. SYSTEM LEVEL OPTIMISATION

### *A. Introduction*

The aim of this project is to maximise the speed of a fishing kayak under human and motor power. Fishing kayaks are used to get out to remote lake and sea fishing locations and use motor power to get most of the distance, followed by a paddle power to get to the desired fishing locations almost silently.

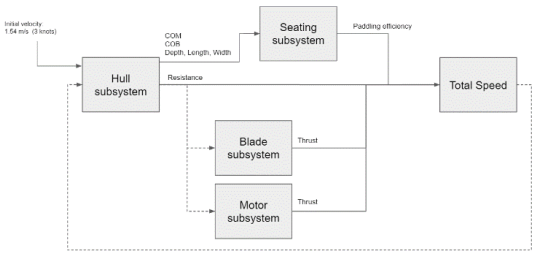


Fig. 1. System relationships

Fishing kayaks are often slow and unwieldy. Our user wants a much faster kayak so they can maximise the time they can fish for. By optimising the system, a better experience can be provided for them. Considering the kayak is to be used in a professional fishing scenario, the cost of production can be neglected in order to achieve maximum efficiency. This report looks specifically into the operation of a fishing kayak on a still flat lake water under motor and paddling power separately. Four subsystems were chosen and optimised for speed. Each subsystem links with one-another, creating a connected system level optimisation.

Expected trade-offs are that with increased speed comes more resistance, lower manoeuvrability, higher fatigue, shorter battery life and lower stability.

Previous work in this area focused on optimisation of racing kayaks and not on the more specialised fishing kayak design. Our aim is to have holistic design suggestions for future fishing kayak products, improving on current designs.

### *B. System Level problem*

#### *1) Assumptions*

Assumptions were made that are used throughout the optimisation. The kayak user was modelled as an average strengthen man weighing 75kg and capable of outputting 125N of peak paddling force. The water was assumed to have no waves or currents. Water was assumed to be fresh water at 20°C with a density of $1000\,kg/m^3$, and a kinematic viscosity of $1.004 \times 10^{-6}$. The kayak was assumed to have no cost limits.

#### *2) System level formulation*

The system level formulation maximises velocity by finding the velocity at which the total resistance of the hull is equal to the maximum total thrust from either the paddle or the motor at any given moment.

Resistance and thrust of the hull are both dependent on the velocity of the boat. As power is transferred as thrust, velocity increases, which increases resistance. When thrust is larger than resistance, the boat accelerates. Velocity reaches its maximum when thrust is equal to the resistance. Velocity, therefore, needs to be found iteratively.

$$V_s = V_s\max \tag{1.1}$$

when

$$F_{\text{paddle}}\max = R_t \tag{1.2}$$

Or

$$F_{\text{motor}}\max = R_t \tag{1.3}$$

#### *3) Subsystem breakdown*

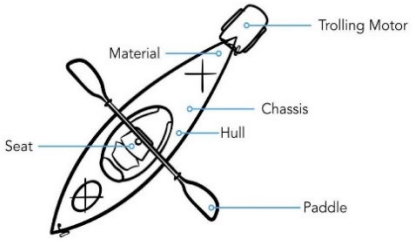


Fig. 2. Subsystem breakdown

The hull subsystem creates resistance that counteracts the trust from the paddle and motor. The paddle subsystem maximises the propulsive efficiency of the paddler based on its muscular strength and the length of the route. The objective for the motor subsystem was to maximise thrust, a reactional force that pushes the boat. The objective of the final subsystem is to maximise the seat height for paddling efficiency, while ensuring boat stability.

## II. SUB SYSTEM 1 – HULL OPTIMISATION

### A. Introduction

#### 1) Summary

This subsystem looks at the optimisation of a fishing kayak hull. Three methods are used to find optimal shape, starting from a simplified macroscopic analysis of dimensions and progressing to a more focused feature-based optimisation. A linear resistance optimisation was performed analytically, then a multi-objective optimisation analysis took both linear resistance and manoeuvrability into consideration. Finally, a manual genetic algorithm was performed using CFD to optimize possible features [1][2].

#### 2) Context

Resistance of a boat hull increases as velocity of a boat increases. [3] The maximum thrust of the boat can generally be considered fixed. Reducing the boat's resistance will increase the maximum speed at which the thrust matches the resistance. Resistance of the ship is a function of the hull shape and velocity, where an increase in velocity of the ship ($V_s$) increases the boat's resistance[4].

### B. Subsystem modelling

The total resistance of the hull can be modelled with the formula:

$$R_t = R_v + R_w + R_{aa} \tag{2.1}$$

The viscous hull resistance $R_v$ can be modelled mathematically, whilst wave-making resistance $R_w$ is derived empirically. A constraint derived from the Froude ratio[1] reduces the effect of $R_w$. Wave making resistance is therefore not considered in this study.

#### 1) Assumptions

The hull's general shape is approximated to a half ellipsoid for mathematical modelling of the system and for the simplification of comparison between mathematical and computation models.

Air resistance ($R_{aa}$) of the hull is also assumed to be negligible as the air resistance of the user is much greater than the hull's resistance.

$R_v$ was derived from first principles and simplified, leading to this equation:

$$R_v = 2\rho {V_s}^2 \pi \left(\frac{(LB)^{1.6} + (LD)^{1.6} + (BD)^{1.6}}{3}\right)^{\frac{1}{16}} \left(\frac{0.075}{\left(log_{10}\left[\frac{LV_s}{1.004\times 10^{-6}}\right] - 2\right)^2}\right) \tag{2.2}$$

#### 2) Variables

The variables for the two mathematical models are:

TABLE I. LIST OF VARIABLES USED IN OPTIMIZATION.

| Name | Symbol | Unit |
|---|---|---|
| Length | ***L*** | N |
| Beam (width) | ***B*** | N |
| Depth | ***D*** | N |
| Profile | ***T*** | $m^2$ |

The CFD based model uses parametric modelling, and the list of variables greatly increases. There are many thousands of possible parameters and values but 6 have been chosen for this optimisation.

| Variable parameter | Discretised values |
|---|---|
| No. of holes | 1, 3, 5 |
| Size of holes | 30mm, 50mm, 70mm |
| Hole flow shielding | 30mm, 50mm, 70mm |
| Hull cross section profile | Straight, Mid, Outer |
| Number of ribs | 1, 3, 5 |
| Depth of ribs | 100mm, 150mm, 200mm |

#### 3) Constraints

The constraints for this subsystem have been derived from both internal and external factors. Internal factors are derived from the user such as minimum depth, width, volume and centre of mass. External factors are dictated by mechanics and include stability and rotational drag.

There are many additional constraints on the hull of a boat that have been excluded from this optimisation, such as manufacturability, cost and transportation.

The constraints were derived from first principles. They were then converted into negative null form:

TABLE II: CONSTRAINTS USED THROUGHOUT MATHEMATICAL OPTIMISATION.

| Constraint | Description | Negative null form | |
|---|---|---|---|
| $g_1$ | Froude ratio | $0.55691\, V_s - L \leq 0$ | (2.3) |
| $g_2$ | X-axis inertia | $\frac{0.3151}{23} - B^2 - D^2 \leq 0$ | (2.4) |
| $g_3$ | Z-axis inertia | $L^2 + B^2 - \frac{4.622}{23} \leq 0$ | (2.5) |
| $g_4$ | Cross-section length | $\sqrt{B^2 + D^2} - T \leq 0$ | (2.6) |
| $g_5$ | Volume | $0.350 - \frac{2}{3}\pi LBD \leq 0$ | (2.7) |
| $g_6$ | Seating depth | $0.2 - D \leq 0$ | (2.8) |
| $g_7$ | Rotational resistance | $162 - 18.18\, L^{3.1} C_d \leq 0$ | (2.9) |

#### 4) Single- objective formulation

TABLE III. FORMULATION FOR SINGLE OBJECTIVE OPTIMIZATION.

| | | | |
|---|---|---|---|
| Min | | $F(x) = R_t(x)$ | (2.10) |
| s.t | $g_1$ | $\frac{0.3151}{23} - B^2 - D^2 \leq 0$ | (2.11) |
| | $g_2$ | $L^2 + B^2 - \frac{4.622}{23} \leq 0$ | (2.12) |
| | $g_3$ | $\sqrt{B^2 + D^2} - T \leq 0$ | (2.13) |
| | $g_4$ | $0.350 - \frac{2}{3}\pi LBD \leq 0$ | (2.14) |
| | $g_5$ | $0.2 - D \leq 0$ | (2.15) |
| | $g_6$ | $162 - 18.18\, L^{3.1} C_d \leq 0$ | (2.16) |

A single objective formulation was created. The additional constraint $g_6$ was derived from first principles and required the calculation of the coefficient of friction ($C_f$). $C_f$ was derived from modelling an equation for the hull shape from empirical data of ellipsoids.

#### 5) Multi-objective formulation

Multi-objective formulation allows for the analysis of the trade-off between resistance during turns ($R_{\mathrm{rot}}$) and total hull resistance for movement in a straight line ($R_t$). This requires additional formulation and the releasing of $R_{\mathrm{rot}}$ as a constraint.

$$R_{\text{rot}} = 18.18\, L^{3.1} C_d \tag{2.17}$$

$$C_d = 2.51 + \exp\left(-0.998\frac{L}{D}\right) + 0.2716 \tag{2.18}$$

$R_{\text{rot}}$ is derived from first principles from the general frictional drag relationship. The coefficient of friction ($C\_d$) is derived from empirical data for flow over similar forms, the meta-model is found *(2.18)* with an adjusted R-square value of 0.9906.

An arbitrary constraint is applied to L of 5m to make sure the problem is constrained.

TABLE IV. FORMULATION FOR MULTI OBJECTIVE OPTIMIZATION.

| | | | |
|---|---|---|---|
| Min | | $F(x) = w_1 R_t(x) + w_2 R_{rot}(x)$ | (2.19) |
| s.t | $g_1$ | $\frac{0.3151}{23} - B^2 - D^2 \leq 0$ | (2.20) |
| | $g_2$ | $L^2 + B^2 - \frac{4.622}{23} \leq 0$ | (2.21) |
| | $g_3$ | $\sqrt{B^2 + D^2} - T \leq 0$ | (2.22) |
| | $g_4$ | $0.350 - \frac{2}{3}\pi LBD \leq 0$ | (2.23) |
| | $g_5$ | $0.2 - D \leq 0$ | (2.24) |
| | $g_6$ | $5 - L \leq 0$ | (2.25) |

### 6) *Parametric Model*

A parametric model of the hull was created in Rhino, using the Grasshopper plug-in. This model is defined by half ellipsoid equations, matching the mathematical model. General shape can be changed, and hull features added.

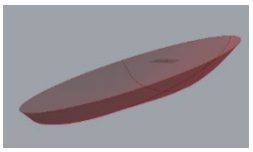

Fig. 3. Plot of length against total hull resistance

### 7) *CFD model*

ANSYS' Discovery Live and Discovery Aim were used for CFD analysis. The 3D model is imported, and a water fluid region created with 4 walls without friction. On the other two walls, water is inlet at 7m/s and outlet at 0 Pa.

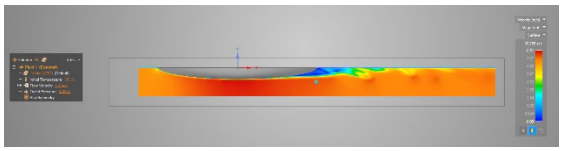

Fig. 4. Flow velocity results of Discovery Live

Discovery Live creates a real time view of fluid velocity and pressure. The setup is exported to Discovery Aim and configuration is perfected. The total hull resistance is then calculated.

Simulations of Linear movement at 7m/s were tested and then a rotational velocity ($\omega$) of 0.154 rad-1 was applied. This simulates an average turn speed during a race. The location of the rotational pivot was approximated to the average paddle position during a turn.

Finally, the model is imported into Aim and the resultant resistive force on the hull surfaces is evaluated.

## C. *Analysis*

### 1) *Monotonicity Analysis*

Monotonicity analysis was performed on the problem to reduce the complexity. Variables were plotted independently against $R_t$. Constraint $g_1$ was found to be inactive and was eliminated.

During single objective optimisation, enough constraints could be eliminated using the first principle of monotonicity (MP1) to allow the objective function to depended only on the length (L). The system could then be optimised by simply choosing the longest kayak that the constraints allow.

TABLE V. MONOTONICITY ANALYSIS

| | | | |
|---|---|---|---|
| Min | $f(L^-, B^+, D^+, T^-)$ | | |
| s.t | $g_1(L^-)$ | (2.26) | |
| | $g_2(B^-, D^-)$ | (2.27) | |
| | $g_3(L^+, B^+)$ | (2.28) | |
| | $g_4(B^+, D^+, T^-)$ | | (2.29) |
| | $g_5(L^-, B^-, D^-)$ | | (2.30) |

### 2) *Single-objective optimisation*

Single objective optimisation of $R_t$ was completed analytically due to the simplicity of the function after the monotonicity analysis.

Length of hull was increased until the maximum allowable by the constraint $g_3$. A longer length was always found to be better at any velocity.

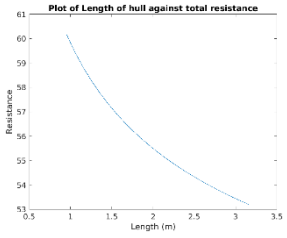


Fig. 5. Plot of length against total hull resistance

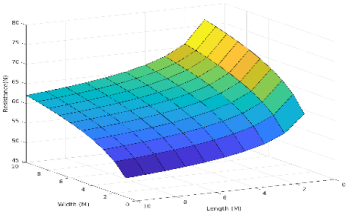

Fig. 6. Plot of Width and Depth against total hull resistance.

### 3) *Multi-objective optimisation*

The pareto set for the multi-objective optimisation was found for the optimisation.

The weighting for the analysis is derived from the optimisation scenario. The hull is turning much less often than it is going in a straight line. The weighting of the optimisation was deemed $w_1 = 2$ and $w_2 = 1$.

Normalisation of Rt and Rrot was completed using the function:

$$f_i^{norm} = \frac{f_i(x) - f_i^{min}}{f_i^{max} - f_i^{min}} \tag{2.31}$$

### 4) *Non-linear solving*

Non-linear solving was performed in Matlab using fmincon's interior points algorithm. This function allows for the solving of problems with non-linear constraints. This was applied to the multi-objective optimisation.

Three variables are upper bounded, and lower bounded. Linear and nonlinear inequality constraints are used but no equality constraints. Initial values are small nonzero values derived from the analytical model.

### 5) *CFD analysis and Genetic Algorithm*

A sensitivity analysis was performed on the design parameters. The most sensitive design parameters were focussed on during the optimisation to reduce the number of samples completed.

A simplified, manual, genetic algorithm was followed. A design was created parametrically and CFD was performed. A fitness value was created from a normalised weighted sum of $R_t$ and $R_{\text{rot}}$. The fitness value was assigned to the each of the parameters. The highest value of each parameter created a child. These were then mutated with the addition of a new parameter.

Automation of the system was deemed too complex for the scope of the project, particularly with integration of such different software.

### D. Optimisation results

#### 1) Mathematical optimisation

TABLE VI. OPTIMISATION RESULTS FOR MATHEMATICAL

| Name | Symbol | Optimised value |
|---|---|---|
| Length | ***L*** | 4.0 m |
| Beam (width) | ***B*** | 0.350 m |
| Depth | ***D*** | 0.20 m |

Initial optimisation showed optimal dimensions were a maximised length and minimised width and depth limited solely by constraints. Maintaining the same manoeuvrability as the benchmark resulted in a maximum length of 4.00 m.

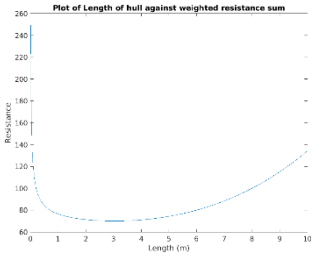


Fig. 7. Plot of Width and Depth against total hull resistance.

During multi-objective optimisation, the weighting between $R_t$ and $R_{\text{rot}}$ was 1000:1, this is because $R_{\text{rot}}$ is for when the boat is static, this number is much small when the boat is in motion and is not at all important. This resulted in a maximum length of 4.0m whilst the width and depth were maintained.

When compared to the benchmark, the optimised boat hull showed an 8.9% decrease in linear hull friction ($R_t$).

#### 2) Computational optimisation

TABLE VII. OPTIMISATION

| Level | Feature | Optimal | Fitness Value |
|---|---|---|---|
| Base | None | NA | 0 |
| 1 | Ribs | 1 Rib, 200 mm depth, Back | 3.205 |
| 2 | Holes | 0 Holes, 0 Shielding, NA | 0 |
| **Total** | | | **3.205** |
| **Final hull Resistance** at 7 m/s | | | **385 N** |
| Rotational hull resistance at 7 m/s | | | **558 N** |

Computational optimisation showed that adding one rib to the back of the boat improved the fitness value of the boat. More ribs were found to increase both the rotational drag and linear drag components. No matter how many holes were added, the small improvements to the rotational components were outweighed by the greatly increased frictional drag components. The optimal kayak hull was found to be one that only had one quite long fin at the back. This had a high fitness value and the system was sensitive to it. This represents a 5% decrease in the weighted linear and rotation hull resistance.

### E. Discussion

Initial exploration of the optimisation problem was performed analytically. This made sense for the simplicity of the model I was working with. There were assumptions that, given more time and resources, could have been used in the optimisation. The assumptions that could have been taken into account would be wave making resistance which accounts for around 30% of total linear hull resistance at the expect velocity. Data would have been gathered on a scale model in a float tank, then a meta-model built. Air resistance could have also been calculated rather than estimated when used to calculate the boat's total resistance.

To account for this, a multiplier of 1.5 times was added to the resistance. This will more than take into account the additional sources of resistance.

During the multi-objective function, the rotational drag equation (2.17) was derived from first principles. It does not take into account the ease of turning when linear motion is applied. A value for the weighting between rotational and linear resistances was chosen so to balance out the two functions. A data driven choice of these weightings would have been better.

The CFD analysis showed a very different total hull resistance than the mathematical model predicted. Large approximations have been made in both models. Despite these differences, comparisons between variables within each model can be made reliably.

The results showed an improvement only in the rib feature. With better features and more complex hull shapes, a CFD analysis would improve both the rotational and linear resistances. This report created the framework for a genetic algorithm that, given more time and resources, could be fully automated. This would allow for a thorough and efficient hull optimisation. The current methodology requires coordination between Grasshopper and ANSYS. A more mathematically driven model that can include features will be necessary for the analysis. I expect that a discretisation of the hull through thin sectional profiles will accommodate this and will be a reliable method for modelling the 3D model mathematically.

### F. Conclusions

When in its simplest form, this optimisation can be solved by simply maximising length and minimising width and depth to the constraints. This was completed using monotonicity. When taking into account manoeuvrability, a multi-objective function using a weighted sub-function found that the optimal length for the boat was 4 m, the width and depth were optimised to 0.2 m deep and 0.35 m wide.

The aim of the project was achieved; however, refinement of the mathematical and computational models would yield more accurate results.

Challenges encountered were many, including deriving new functions from first principles, in the process approximating meta-models for crucial variables. I also had to learn CFD analysis from scratch and create a full and accurate 3D model in order to get a more accurate and flexible analysis, a huge step up in complexity.

Due the challenges of the problem, I learnt a wide cross section of different optimisation techniques.

## III. SUBSYSTEM 2 – PADDLE OPTIMISATION

Three main factors affect the propulsive efficiency of a kayaker: paddling stroke technique, design of the paddle blade, and muscular strength of the paddler [5].
In practice, it should be possible to determine the optimal paddle design and technique that best matches the muscle force-velocity profile of any given kayaker.
The goal of this study is to maximize the propulsive force generated in a specific amount of time.

### *A. Optimisation Formulation*

#### *1) Objective Function*

The main idea of being efficient is to produce thrust with the least energy. A paddle creates lift and drag forces when pulled sideways. These forces vary mostly with the angle of attack of the blade in the water. These forces depend on a few variables and can be written as follow.

Instantaneous force:

$$|\boldsymbol{F_x}| = \frac{1}{2}\boldsymbol{\rho A C_d v^2} + \frac{1}{2}\boldsymbol{\rho A C_l v^2} \tag{3.1}$$

To determine the force generated in a stroke, it is necessary to sum up the instantaneous force at each angle of the stroke:

$$\boldsymbol{force_{stroke}} = \int_{\propto_{in}}^{\propto_f} \frac{1}{2}\boldsymbol{\rho}\left(\boldsymbol{U_{max}}\sin\left(\boldsymbol{\pi}\frac{\propto_f}{\boldsymbol{180}}\right)\right)^2 \boldsymbol{A}\,(\boldsymbol{C_D} + \boldsymbol{C_L}) \tag{3.2}$$

In these equations, $\rho$ represents the density of the water, $A$ the submerged surface area of the blade, $v$ its speed relative to the water (while $U_{max}$ the peak speed), $\propto_{in}$ and $\propto_f$ are the angle of entry and exit of the blade, and $C_l$ and $C_d$ are respectively called the lift and drag coefficients. They mainly depend on the Reynolds number and on the shape of the blade.
As the length of the race increases, the paddler needs to manage their energies. Force profile affected by fatigue:

$$-\boldsymbol{1.5} \times \left(\boldsymbol{n^{\circ}_{strokes}}\right)^2 + \left(\boldsymbol{n^{\circ}_{strokes}}\right)\left(\boldsymbol{force_{stroke}}\right) - \left(\boldsymbol{force_{stroke}} - \boldsymbol{1.5}\right) \tag{3.3}$$

Objective function:

$$\begin{aligned} &-\boldsymbol{1.5} \times \left(\frac{\boldsymbol{180}}{\frac{\boldsymbol{Travel}}{\boldsymbol{U_{max}}} + \boldsymbol{0.2}}\right)^2 \\ &+ \left(\frac{\boldsymbol{180}}{\frac{\boldsymbol{Travel}}{\boldsymbol{U_{max}}} + \boldsymbol{0.2}}\right)\left(\int_{\propto_{in}}^{\propto_f} \frac{1}{2}\boldsymbol{\rho}\left(\boldsymbol{U_{max}}\sin\left(\boldsymbol{\pi}\frac{\propto_f}{\boldsymbol{180}}\right)\right)^2 \boldsymbol{A}\,(\boldsymbol{C_D} \right. \\ &\left. + \boldsymbol{C_L})\,\boldsymbol{d}\propto_f\right) \\ &-\left(\int_{\propto_{in}}^{\propto_f} \frac{1}{2}\boldsymbol{\rho}\left(\boldsymbol{U_{max}}\sin\left(\boldsymbol{\pi}\frac{\propto_f}{\boldsymbol{180}}\right)\right)^2 \boldsymbol{A}\,(\boldsymbol{C_D} + \boldsymbol{C_L})\,\boldsymbol{d}\propto_f - \boldsymbol{1.5}\right) \end{aligned} \tag{3.4}$$

#### *2) Design Variables*

The three design variables of the paddle system are the maximum paddle blade velocity (Umax), the surface area of the blade ($A$), and the angle of exit of the paddle during the stroke ($\propto_f$).
As the velocity and the area increase, the force generated by the blade increases. But a higher velocity means more strokes, which leads to a higher effort and fatigue for the paddler.
As the angle of exit increases, the force generated during the stroke increases, but it also takes more time, reducing the number of total strokes doable in a specific amount of time.

TABLE X. VARIABLES

| $x$ | Description | Unit |
|---|---|---|
| $A$ | Paddle's Blade Surface Area | $m^2$ |
| $U_r$ | Peak Blade Tangential Velocity | $m/s$ |
| $\propto_f$ | Stroke Exit Angle of blade | $degrees(°)$ |

#### *3) Design Constraints*

The design constraints in this study include physical and functional constraints. Physical constraints will ensure the paddle blade dimensions are manageable by the paddler.
Functional constraints are related to the stroke technique of the paddler. These can be found in Table 2 below.

TABLE XI. CONSTRAINTS

| $g_x$ | Description |
|---|---|
| $g_1$ | Angle of exit of the blade is bigger than 25° |
| $g_2$ | Angle of exit of the blade should not exceed 180° |
| $g_3$ | The force required to move the paddle should be less than the paddler's maximum strength |
| $g_4, g_5$ | The surface area of the blade should be between the specified values used in industry |
| $g_6$ | The number of strokes shouldn't exceed the rate of 180 strokes/min |
| $g_7$ | The blade peak velocity should always have positive values |

The following assumptions were made to simplify the complexity of the model:

- Pitch and Roll motion of the blade are neglected
- The sea water has no waves or currents
- The blade surface is always completely underwater during the stroke
- The Paddling Time is 180 seconds (3 mins)

#### *4) Design Parameters*

Parameters used are:

TABLE X. PARAMETERS

| $g_x$ | Description | Value |
|---|---|---|
| $\propto_{in}$ | Angle of entry of the blade in water | 25° |
| $C_h$ | Chord of the blade surface | 20 $mm$ |
| $\rho$ | Density of Water | 1000 $kg/m^3$ |
| $T_{rec}$ | Time it takes to the paddler to move paddle back to start after each stroke | 0.2 $sec$ |
| $r$ | The radius of curvature of the paddle as it gets rotated in water | 0.5 $m$ |
| $C_D$ | Coefficient of Drag (varies with respect to $\propto_f$) | |
| $C_l$ | Coefficient of Lift (varies with respect to $\propto_f$) | |

#### *5) Model Summary*

$$\begin{aligned} &\min\, f(\mathbf{x}, \mathbf{p}) = -f(x) \\ &= -1.5 \times \left(\frac{180}{\frac{Travel}{U_{max}} + 0.2}\right)^2 \\ &+ \left(\frac{180}{\frac{Travel}{U_{max}} + 0.2}\right)\left(\int_{\propto_{in}}^{\propto_f} \frac{1}{2}\rho\left(U_{max}\sin\left(\pi\frac{\propto_f}{180}\right)\right)^2 A\,(C_D + C_L)\,d\propto_f\right) \\ &-\left(\int_{\propto_{in}}^{\propto_f} \frac{1}{2}\rho\left(U_{max}\sin\left(\pi\frac{\propto_f}{180}\right)\right)^2 A\,(C_D + C_L)\,d\propto_f - 1.5\right) \end{aligned}$$

$$
\begin{aligned}
s.t. \quad & g_1(\propto_f): \propto_f - 180 \leq 0 \\
& g_2(\propto_f): 25 - \propto_f \leq 0 \\
& g_3(A, U_{max}): \frac{1}{2}\rho A C_d {U_{max}}^2 - 125 \leq 0 \\
& g_4(A): 0.003 - A \leq 0 \\
& g_5(A): A - 0.009 \leq 0 \\
& g_6(A): \frac{180}{\frac{(\propto_f - 25) \times 0.0175 \times r}{U_{max}} + 0.2} - 180 \leq 0 \\
& `g_7(U_{max}): -U_{max} \leq 0
\end{aligned}
$$

### B. Modelling Approach

The modelling approach table in the Appendix gives an overview of the way different parts of the same function have been derived.

The instantaneous force was derived from first principles, but the parameters $C_D$ and $C_L$ are coefficients that depend on the orientation of the blade in water and on the shape of the blade.

The Force-fatigue profile of the paddler was a metamodel derived from data extrapolated from previous studies.

The only active constraint, the one related to the maximum strength of the paddler, was derived through 1st principles.

#### 1) Drag & Lift Coefficients

Since the lift creates the thrust and the drag is related to the strength of the athlete, the design should minimize the drag and maximize the lift [6]. Instead than designing an infinite number of shapes and evaluate their drag and lift coefficients, a shortcut has been taken for this project. The Reynolds number of the blade in the water is of the order of magnitude of 106, similar to the one of an airplane wing. The NASA has been filling in a database of foils, where they measured the lift and the drag created for every angle of attack.
The coefficients' data for the airfoil with the highest lift to drag ratio was used as an input for the MatLab function polyfit(x,y,n), in order to find the coefficients of a polynomial p(x) of degree n that fitted the data.

The airfoil with the highest ratio resulted to be the GOE 448 Airfoil.

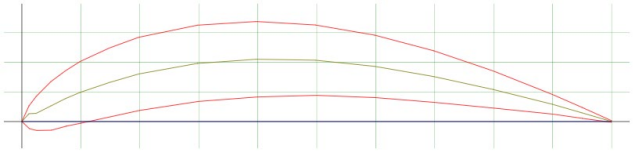

Fig. 8. GOE 448 Airfoil Section Profile

A metamodel was then generated from the coefficients data related to this specific airfoil, giving the equations below.

$$C_D = 2.9e^{-8} \propto_f^4 - 1.07e^{-5} \propto_f^3 + 0.001 \propto_f^2 - 0.005 \propto_f - 0.0004 \quad (3.5)$$

$$C_L = 1.6e^{-8} \propto_f^4 + 1.05e^{-5} \propto_f^3 - 0.002 \propto_f^2 + 0.077 \propto_f + 1.01 \quad (3.6)$$

#### 2) Peak Force – Strokes Relationship Model

A study conducted on physiological responses of Kayak athletes identified significant negative correlations between the number of strokes and the peak force [7].
This linear regression model was used to estimate the effects of the number of strokes on the force efficiency. In fact, as the number of strokes increases, the fatigue will increase.
Data was extrapolated from that graph, imported in MATLAB and fitted with a metamodel. This metamodel was then integrated across the number of strokes to obtain a Force profile metamodel.

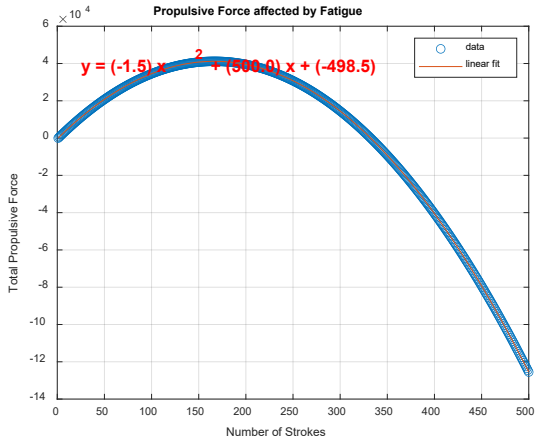


Fig. 9 Propulsive Force Profile affected by Fatigue

#### 3) Maximum Strength Constraint

As when both the velocity and the area of the blade increase, the force increases, the only limit is the actual maximum force that the paddler would handle.

Instantaneous force:

$$|F_x| = \frac{1}{2}\rho A C_d v^2 + \frac{1}{2}\rho A C_l v^2 = \frac{1}{2}\rho \left(U_{max} \sin\left(\pi \frac{\propto_f}{180}\right)\right)^2 A (C_D + C_L) \quad (3.7)$$

The maximum force value during the stroke will happen at $\propto_f = 90$, where $C_D = 1.8$ and $C_L = 0$

$$|F_x| = \frac{1}{2}\rho (U_{max})^2 A (1.8) = 900 (U_{max})^2 A \quad (3.8)$$

Based on … paper, an average paddler's maximum force was assumed to be 125 N, therefore:

$$900 (U_{max})^2 A \leq 125 \qquad A \leq \frac{125}{900 (U_{max})^2} \qquad A \leq \frac{1}{7.2 (U_{max})^2} \quad (3.9)$$

### C. Explore the Problem Space

#### 1) Monotonicity Analysis

From the monotonicity table below we can see that all the variables are well bounded since they have an upper and lower bound. There is uncertainty about the monotonicity sign for

the variables $\propto_f$ and $U_{max}$ in the objective function since the function follows a non-linear path as the variables increase.

| State | Number | Equation | $U_{max}$ | $A$ | $\propto_f$ |
|---|---|---|---|---|---|
| | $-f(x)$ | | ? | − | ? |
| **Semiactive** | $g_1(x)$ | $25 - \propto_f \leq 0$ | | | + |
| **Semiactive** | $g_2(x)$ | $\propto_f - 180 \leq 0$ | | | − |
| **Active** | $g_3(x)$ | $900{U_{max}}^2 A - 125 \leq 0$ | + | + | |
| **Semiactive** | $g_4(x)$ | $0.005 - A \leq 0$ | | − | |
| **Semiactive** | $g_5(x)$ | $A - 0.015 \leq 0$ | | + | |
| **Inactive** | $g_6(x)$ | $Stroke\ Rate - 180 \leq 0$ | + | | − |
| **Semiactive** | $g_7(x)$ | $-U_{max} \leq 0$ | − | | |

### D. Optimisation

#### 1) Algorithms Analysis

The objective function was plotted on a 3-dimensional graph to investigate its shape and the potential risks.

The variables used in this study were continuous, so a continuous solver such as fmincon was used.

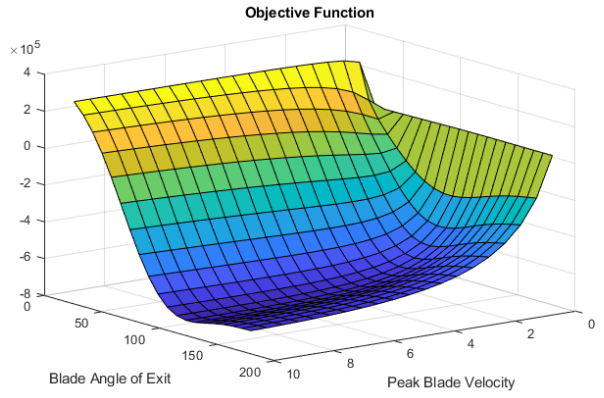


Fig. 9. Objective Function 3D Plot

#### 2) Fmincon Interior Point Algorithm

The MATLAB fmincon algorithm was used to determine the local minima of the function. This is because it can be simple to implement and fast for solving constrained optimisation problems.

The results showed that an exit angle of 124.9° and a paddling velocity of 4.4 m/s would produce the highest propulsion from a paddler with a 125 N maximum arm strength. The run time was found to be 3.52 seconds.

#### 3) Fmincon Sequential Quadratic Programming Algorithm

Fmincon sqp was then used to test reproducibility and validate the results. It produced the same optimal values but had an improved run time of 3.15 seconds. This behaved as expected as sqp is not a large-scale algorithm.

#### 4) Global Search

A problem with fmincon interior points is that it can become stuck at a local minimum. It was therefore checked for robustness using GlobalSearch to determine the global minimum. It provided the same results with 11 local solver runs converging with a positive local solver exit flag.

#### 5) Results

The results of the optimisation algorithm showed an exit angle of 124.9°, and a maximum paddling velocity of 4.4 m/s. By feeding back these results into the other variables, the results are a blade surface area of 70.6 $cm^2$ and a stroke rate of 151 strokes/min.

The total propulsive force along the whole 180 seconds of 1,235,409 N.

Fmincon sqp was the most computationally inexpensive algorithm that provided the same optimal values and met all conditions.

TABLE XI. RESULTS

| | |
|---|---|
| Maximum Velocity | 4.4 m/s |
| Stroke Exit Angle | 124.9° |
| Surface Area | 70.6 $cm^2$ |
| Total Propulsive Force | 1,235,409 N |
| Stroke Rate | 151.3 strokes/min |
| Number of Strokes | 453.8 |
| Average Thrust | 58.8 N |

### E. Discussion

#### 1) Sensitivity Analysis

The Lagrange Multipliers structure was analysed to determine the sensitivity at the upper and lower bounds of the variables. These values, reporting an order of magnitude of $10^3$ and $10^4$ , are effectively zero, indicating that the solution is not near the bounds.

An interesting aspect to evaluate was to see is how the two variables change with the paddling time, set at 180 seconds for the optimisation.

#### 2) Not Accounting for Fatigue

When reshaping the objective function to not take into account fatigue, the results of the optimisation suggest a shorter stroke (118°) and the maximum possible blade velocity (5 m/s, the upper bound set). This because a higher velocity in water increases both force and stroke rate.

#### 3) Scaling

The surface area variable, A, had an order of magnitude of $10^{-3}$, way lower compared to $10^2$ and $10^1$ of respectively the Exit Angle and Max Velocity variables. But having got rid of the surface area variable through the substitution of the active constraint, there was no need for scaling.

#### 4) Uncertainty & Further Development

The optimum value for the variables depends mainly on the paddler's muscular strength and the paddling time. Therefore, in order to proceed with a suggestion for a specific paddler, it's important to first accurately evaluate the maximum strength that the paddler can push and the approximate time he is planning to paddle for.

To conclude, it's difficult to evaluate the improvements of this optimisation compared to benchmark values as there aren't any specific results for a paddler with 125 N maximum paddling strength. However, the results of this study showed a suggested stroke rate in the same range as world kayak medallist (139-159 strokes/min) [8].

## IV. SUBSYSTEM 3 - TROLLING MOTOR

A trolling motor is made up of two main components, a propeller and a motor. The power developed by a trolling motor is available at the propeller shaft in the form of torque. This torque is then converted into thrust, a reactional force caused by a pressure differential that pushes the boat, Figure 10 [3][9]. The objective for this subsystem was to maximise this thrust force.

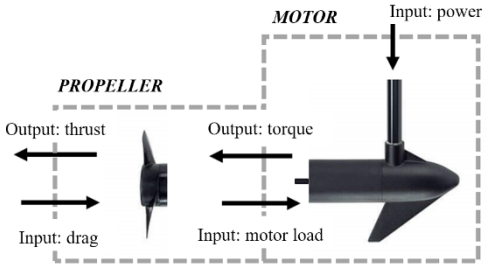


Fig. 10. System decomposition of a trolling motor [10].

The thrust created by a trolling motor, is affected by variables relating to the motor and propeller design. The following section will elaborate on the modelling of thrust using first principles and empirical correction factors, as well as the methods used to identify optimum quantities for variables such as propeller pitch, propeller diameter, blade number, chord length and voltage provided to motor; in order to maximise thrust while meeting functional criteria (constraints).

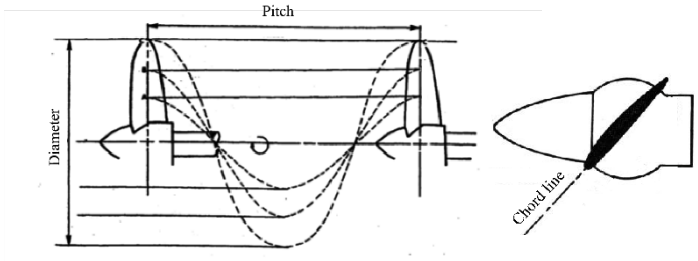


Fig. 11. Typical propeller operating through one revolution (left). Diagram with chord line annotated (right) [11].

### A. *Optimisation formulation*

Below is are the constraints, parameters and objective function presented in its negative null form. On a subsystem level resistive force of the boat and drag force from the boat was not considered.

$$\min\ f(\mathbf{x},\mathbf{p}) = F_{\text{motor}} = -3.859\ x\ 10^{-12}\ \pi\rho(K_v v)^2 d^{3.5}\sqrt{p} \quad (4.1)$$

$$\textbf{where} \quad \mathbf{x} = (d,p,v,b,c) \quad \in \chi \in \mathbb{R}^n \quad (4.2)$$

$$\mathbf{p} = (\rho, Kv) \quad (4.3)$$

$$\textbf{s.t.} \quad h_1(\rho) = \rho - 1000 = 0 \quad (4.4)$$

$$h_2(Kv) = K_v - 150 = 0 \quad (4.5)$$

$$g_1(p,d) = 0.85 - p\ /\ d \le 0 \quad (4.6)$$

$$g_2(p,d) = p\ /\ d - 1.5 \le 0 \quad (4.7)$$

$$g_3(d,b,c) = 0.35 - bc\ /\ \pi d \le 0 \quad (4.8)$$

$$g_4(v) = 12 - v \le 0 \quad (4.9)$$

$$g_5(v) = v - 24 \le 0 \quad (4.10)$$

$$g_6(b) = 1 - b \le 0 \quad (4.11)$$

$$g_7(b) = b - 3 \le 0 \quad (4.12)$$

$$g_8(c) = 1 - c \le 0 \quad (4.13)$$

$$g_9(c) = c - 4 \le 0 \quad (4.14)$$

$$g_{10}(p) = 1 - p \le 0 \quad (4.15)$$

$$g_{11}(p) = p - 10 \le 0 \quad (4.16)$$

$$g_{12}(d) = 1 - d \le 0 \quad (4.17)$$

$$g_{13}(d) = d - 12 \le 0 \quad (4.18)$$

Below are the chosen design variables and their relationships with thrust force and the other variables, Table XII.

TABLE XII. TABLE OF DESIGN VARIABLES

| Variable | Symbol | Description of relationship with thrust and other variables | Source |
|---|---|---|---|
| ***Propeller Diameter (Inches)*** | *d* | The propeller diameter is proportional to the thrust produced, as a larger diameter distributes more power and thrust on a larger volume of fluid. | [12] |
| ***Pitch Length (Inches)*** | *p* | The pitch effectively converts torque to thrust, it determines how far you move as a single rotation (Figure 11). The pitch has effect on the revolutions per minute (RPM). The ratio between the pitch and diameter is also crucial for the functionality of the propeller. | [9][13] |
| ***Voltage (V)*** | *v* | The voltage supplied to the motor is proportional to both RPM of the motor as well as the power supplied to the motor; therefore, proportional to the thrust generated by the motor. | [14] [15] |
| ***Blade number*** | *b* | The blade number is related to the solidity of the propeller, rotor solidity ratio, a ratio which also incorporates the diameter of the propeller. Increasing the blade number increases the surface area to propel against fluid, therefore maximising the thrust produced. | [16] |
| ***Chord length*** | *c* | The chord length influences the rotor solidity as the efficiency of the propeller. Viscous losses also scale with chord length. Chord line is shown on Figure 11. | [12] [16] [17] |

### B. *Modelling approach and assumptions*

#### 1) *Objective equation formulation*

Considering Newton's second law, we can define the thrust force ($F_{\text{motor}}$) to be the change in momentum of an object, momentum is an object's mass (m) times it's velocity ($V$). The change in velocity ($\Delta V$) is shown by velocity of exit($V_e$) subtracted from the freestream velocity($V_f$) (4.19) [18][19].

$$F_{\text{motor}} = m\Delta V = m(V_e - V_f) \quad (4.19)$$

For a moving fluid it is important that we incorporate the mass flow rate ($m_{dot}$), which is the amount of mass moving through a given plane over a certain amount of time. This is equal to the cross-sectional area (A) through which the fluid is flowing times the velocity of the fluid ($V_e$), multiplied by density of freshwater ($\rho$). Where rotor disc area (A) is simplified to the area of a circle (4.20) [17][19].

$$m_{dot} = \rho A V_e = \rho \frac{\pi d^2}{4} V_e \quad (4.20)$$

By substitution we get the following equation (4.21) which summarises theoretical dynamic propeller thrust.

$$F_{\text{motor}} = \rho \frac{\pi d^2}{4} V_e (V_e - V_f) \tag{4.21}$$

Pitch speed ($V_p$) is a function of RPM of the propeller as well as pitch ($p$), which represents the theoretical distance forward that the propeller moves in one revolution, equation (4.22). The propeller travels at pitch speed when the propeller is most efficient. Using this assumption and conversion rates we can deduce equation (4.22) [19][20].

$$V_p = 0.000423\, p\, RPM \tag{4.22}$$

Equation (4.21) can be simplified to static thrust, which incorporates design variables that the designer can change; by substituting pitch speed for exit velocity and equating free stream velocity to 0, as well as incorporating conversion multipliers for diameter (4.23).

$$F_{\text{motor}} = \rho \frac{\pi (0.0254\ d)^2}{4} (0.000423\, p\, RPM)^2 \tag{4.23}$$

Calculating dynamic thrust is highly dependent on inflow velocity, pressure changes and often it is calculated using momentum theory which greatly simplifies the design parameters of a propeller to the diameter or area of propeller [3][21]. Due to this a static thrust equation was used. Through use of correction factors based on empirical data, a thrust equation can be obtained that is seen as accurate within +/- 26% of a most cases (at high speeds) [14][19][22].

Equation (4.24) is the objective equation in its negative null form, with the motor velocity constant ($K_v$) and voltage ($v$) substituted for RPM and empirical correction factors incorporated. A coefficient of 0.8 was also incorporated, assuming the efficiency of the propeller is 80% [22][23]. This equation was then simplified (4.1).

$$F_{\text{motor}} = -0.8\, \rho \frac{\pi (0.0254\, d)^2}{4} (0.000423\, p\, K_v\, v)^2 \left(\frac{d}{3.29546\, p}\right)^{1.5} \tag{4.24}$$

### 2) *Design constraints and parameters*

Constraints were used to bound variables, as well as incorporating further functional design criteria, for example maintaining a suitable value for the rotor solidity ratio ($g_3$).

TABLE XIII. FUNCTIONAL CONSTRAINT TABLE

| Constraint | Constraint description, assumptions and tradeoffs | Source |
|---|---|---|
| $\boldsymbol{g_1(p,d)}$ | Pitch to diameter ratio constraint. Created to reduce likelihood of stalling and ensure pitch ratio is within optimal range. | [12] [13] |
| $\boldsymbol{g_2(p,d)}$ | Pitch to diameter ratio constraint. Created to ensure trolling motor is within suitable shaft speed and ensure pitch ratio is within optimal range. | [9] |
| $\boldsymbol{g_3(d,b,c)}$ | Rotor solidity constraint. Created to improve rotor solidity and reduce risk of cavitation. | [24] |
| $\boldsymbol{g_4, g_5(v)}$ | Voltage bounding. Informed by motor voltages on the market (benchmarking) that voltage values would work with available circuit breakers. | [25] [26] |
| | Maximum 24V constraint ensures that kayak isn't travelling at unsafe speeds for our boat length and assumed weight. | |
| $\boldsymbol{g_6, g_7(b)}$ | Blade number bounding. A propeller with more blades will perform better however and increase surface area in contact with the fluid, however more blades means reduced chord which can cause issues with cavitation and fatigue. | [12][16] |
| $\boldsymbol{g_8, g_9(c)}$ | Chord length bounding. Large chord lengths can help reduce cavitation however reduce efficiency of a propeller due to viscous losses. Minimum chord length to allow for blade solidity and reduce cavitation. | [17] |
| $\boldsymbol{g_{10}, g_{11}(p)}$ | Pitch bounding. Large pitch may have good efficiency, but blades tend to stall. A large pitch will also reduce RPM however a small pitch can also ruin the engine. | [9][12] |
| $\boldsymbol{g_{12}, g_{13}(d)}$ | Diameter bounding. Similar bounding to pitch as a propeller with the same pitch and diameter length is most efficient. Maximum value diameter is larger than pitch as it is more important to absorb torque. The diameter range is also similar to propellers on the market (benchmarking). | [9] [19] |

TABLE XIV. PARAMETER TABLE

| Constraint | Constraint description and assumptions | Source |
|---|---|---|
| $\boldsymbol{h_1(\rho)}$ | Density of freshwater is 1000 kg/m$^3$ | [2] |
| $\boldsymbol{h_2(K_v)}$ | Motor velocity constant was assumed to be 150, based on motor data and forums (benchmarking). | [23] |

Alongside previously mentioned assumptions the following subsystem assumptions were also considered, Table XV.

TABLE XV. ADDITIONAL SUBSYSTEM ASSUMPTIONS

| No. | Descriptions | Source |
|---|---|---|
| 1 | The propeller imparts a uniform force to the water passing through it. | [3] |
| 2 | The thrust generated by propeller is uniformly distributed over the entire disk. | [3] |
| 3 | The flow is frictionless. | [3] |
| 4 | There is an unlimited supply of water available to the propeller. | [3] |
| 5 | The propeller effeciency was assumed to be 80% rather than a function of thrust, diameter, speed etc. | [9] [12] |
| 6 | Drag force, viscous losses and resistive force of the boat were not considered when maximising thrust, beyond the incorporation of 80% efficiency. | |
| 7 | $K_v$ was assumed to be constant. | [23] |
| 8 | Pitch length did not affect the RPM ($K_v$v) of the propeller | [9] |
| 9 | The fundamental principles behind airplane and marine propellers are the same (except for the difference in fluid densities). | [23] |

## C. *Exploring the problem space*

Monotonicity of the objective and constraint functions were exploited in order to reduce the problem space and check the minimisation problem is well-bounded, Table XVI. The non-active constraints were eliminated, and voltage was solved to be 24V.

TABLE XVI. MONOTONICITY TABLE

| Function | Design variables | | | | | Active |
|---|---|---|---|---|---|---|
| | $d$ | $p$ | $v$ | $b$ | $c$ | |
| $f$ | - | - | - | | | |
| $g_1(p,d)$ | + | - | | | | *Yes* |
| $g_2(p,d)$ | - | + | | | | *Yes* |
| $g_3(d,b,c)$ | + | | | - | - | *Yes* |
| $g_4(v)$ | | | - | | | *No* |
| $g_5(v)$ | | | + | | | *Yes* |
| $g_6(b)$ | | | | - | | *No* |
| $g_7(b)$ | | | | + | | *Yes* |
| $g_8(c)$ | | | | | - | *No* |
| $g_9(c)$ | | | | | + | *Yes* |
| $g_{10}(p)$ | | - | | | | *No* |
| $g_{11}(p)$ | | + | | | | *Yes* |
| $g_{12}(d)$ | - | | | | | *No* |
| $g_{13}(d)$ | + | | | | | *Yes* |

## D. *Optimisation*

The minimisation problem was optimised using MATLAB's fmincon. Constrained non-linear gradient-based methods called Sequential Quadratic Programming algorithm (SQP) and Interior Point were used. Both methods use quasi-Newton methods and identify local minimums.

MATLAB'S GlobalSearch was used to identify if the minimums produced were global minimums.

TABLE XVII. RESULTS TABLE

| Algorithm | Optimal value | | | | Performance |
|---|---|---|---|---|---|
| | *diameter* | *pitch* | *blade number* | *chord* | *Time (s)* |
| ***SQP*** | 10.588 | 9 | 3 | 4 | 1.519 |
| ***Interior Point*** | 10.588 | 9 | 2.989 | 3.9844 | 1.945 |
| ***Global Search*** | 10.588 | 9 | 2.976 | 3.918 | 5.298 |

All three algorithms converged to the same optimal values when rounded to one decimal place (Table XVII) and outputted the final optimal thrust value to be 1820.679 N, using the voltage value of 24V which was solved using monotonicity analysis.

Following the optimisation, sensitivity analysis was performed. This was done by examining the Lagrange multipliers (returned after SQP and Interior Point optimisation). It seems the parameter $K_v$ had a relatively high Lagrange multiplier (24.276, 3rd largest upper bound multiplier). Previously, it was decided to assume the value in order to simplify the optimisation problem, despite knowing that the constant $K_v$ may vary as voltage changes. The Lagrange multiplier value emphasises to the need to reconsider assuming a value for this parameter.

This statement is further emphasised by Figure 12, which indicates the parametric plots of pitch and potential $K_v$ values, illustrating that given the potential $K_v$ range and pitch range, $K_v$ could have more impact on the output thrust.

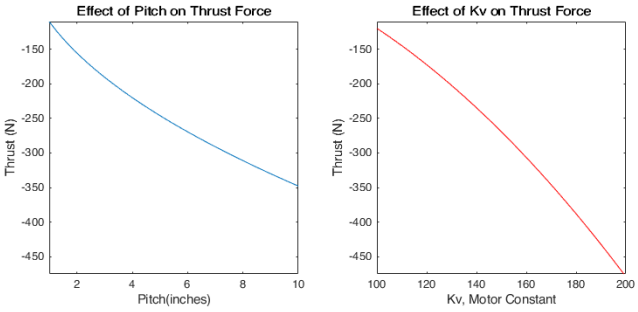


Fig. 12. Parametric plot comparison of pitch and $K_v$

## E. *Discussion*

In terms of the algorithm performances, the Global Search solver was most computationally expensive, as suspected; as it identifies a local minimum and explores for other start points that are likely to improve the best local minimum. Whereas both SQP and Interior Points only identify local minimums. In addition to this, the SQP algorithm was the most computationally inexpensive as it takes larger steps in the optimisation process. Based on performance and results, SQP was the most effective algorithm.

A challenge was formulating a representative yet simple model to optimise. The objective function was derived from large assumptions. For example, assuming pitch speed is equated to exit velocity, assuming efficiency is not a function of the design variables and neglecting drag; these assumptions are not representative of real life [12][19]. In addition to this, the correction factors used are less accurate for slow speed propellers.

Further steps to improve the optimisation problem include:

- Calculating my own empirical correction factors using a propeller test rig, rather than market data and air propeller data.
- Incorporating the relationship between the design variables and drag.
- Incorporating a propeller efficiency equation that is a function of design variables into my objective equation.
- Identifying how $K_v$ can change with different voltage values.
- Investigate further into blade element theory to identify relationships with other variables and thrust, for example pitch angle.

## F. *Conclusion*

Overall the optimisation was successful, as the three algorithms identified consistent logical optimum values. However, the optimisation using the fmincon solvers tended to the upper bounds of the variables, these combinations of variables are less available and are generally more expensive combination of options. Despite being successful from the perspective of a user that has not taken cost into account, this is not representative of most customers of trolling motors.

## V. SUBSYSTEM 4: SEATING POSITION

The seating position of the kayaker affects how easy it is for them to paddle, hence affecting their efficiency and speed. Extensive empirical studies have been done in this field previously, trying to identify dependencies between the seating position and speed or kayaker comfort. Notably, Ong et al. [29] have looked into *examining the inter-relationship between athlete morphology, equipment set-up and performance in elite sprint kayaking.* The study analysed the setups of Olympic kayakers and tried to identify the relationships between foot-bar distance, seat height and paddle grip width and athlete body build. Unfortunately, the models constructed in this study did not prove to increase paddling efficiency in intervention trials.

Looking further, other studies, like the one by Broomfield [30] argue that a higher seat position increases paddling efficiency by making it easier to achieve the optimal paddle entry angle. However, there is a limit to how high the seat can be positioned before it compromises the boat's balance, making it too unstable to control. Considering not much research has been done in this area previously, this subsystem modelling will focus on finding the optimal seat height by applying the rules of ship stability and buoyancy physics.

### A. *Model Formulation*

When discussing ship stability, three main points are identified – centre of gravity, centre of buoyancy and the metacentre. For the ship to be in equilibrium the x and y coordinates (in this case along the width and length of the kayak) of these points have to lie in the centre of the boat. As the design of the kayak hull is symmetrical by nature, we can ignore these components and focus on the z coordinate, or their height.

As stated in Lautrup's textbook [31]: *for the ship to be stable the restoring moment must counteract the tilt […], (this occurs) when the metacenter lies above the center of gravity.* Based on this, $z_M$ can be expressed as:

$$z_M = z_B + \frac{I_0}{V_0} \tag{5.1}$$

Where $I_0$, the second moment of inertia around the x-axis of the hull waterline area $A_0$:

$$I_0 = \int_{A_0} (y - y_0)^2 dxdy \tag{5.2}$$

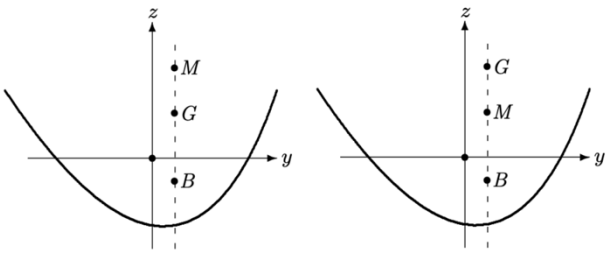


Fig. 13. The relation of the positions of the metacenter (M) and center of gravity (G) for a stable (left) and unstable (right) ship.

Bearing in mind that this problem becomes very complex to model for an ellipsoid shape and the human body, the kayak hull and the person inside it have been simplified to both have a rectangular cross-section. The kayak is modelled to have a height of $2a$ in the z-axis, width of $2b$ in the y-axis and length of $2c$ in the x-axis with a depth of d below the waterline.

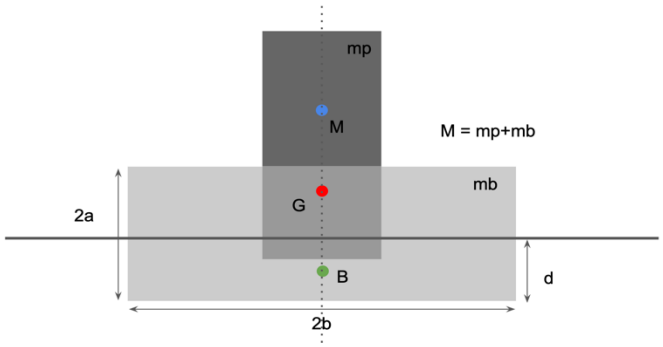


Fig. 14. Cross-section diagram of the human-kayak system.

It is important to remember that the positions of the equilibrium points seen on Figure 14 are for the entire human-kayak system. In the following calculations $M$ is taken to be the mass of the system, or the sum of the mass of the boat ($m_b$) and the mass of the person ($m_p$).

Considering the rules of buoyant equilibrium, the equation for the restoring moment around the x-axis ($\mathcal{M}_x$) in terms of tilt angle ($\alpha$), positions of the centers of buoyancy and gravity in z-axis ($z_B$, $z_G$), the second moment of inertia ($I_0$), displaced volume of water ($V_0$), total mass of human-kayak system ($M$) and gravitational acceleration ($g_0$), can be derived to be:

$$\mathcal{M}_x = -\alpha \left( z_B + \frac{I_0}{V_0} - z_G \right) M g_0 \tag{5.3}$$

For a cuboid kayak shape:

$$I_0 = \int_{-c}^{c} dx \int_{-b}^{b} dy\, y^2 = \frac{4}{3} c b^3 \tag{5.4}$$

$$V_0 = \frac{M}{\rho_0} = 4bcd \tag{5.5}$$

$$z_B = -\frac{d}{2} \tag{5.6}$$

Rearranging (4.3) for $z_G$ and substituting:

$$z_G = \frac{\mathcal{M}_x}{M g_0 \alpha} + z_B + \frac{I_0}{V_0} \tag{5.7}$$

$$z_G = \frac{\mathcal{M}_x}{M g_0 \alpha} + \frac{4cb^3\rho}{3M} - \frac{M}{8\rho bc} \tag{5.8}$$

$$z_G = \frac{24bc\rho\mathcal{M}_x + 32c^2b^4\rho^2 g_0\alpha - 3M^2 g_0\alpha}{24M g_0 \alpha bc\rho} \tag{5.9}$$

### B. *Optimisation Formulation*

Following, is the objective function for the optimisation problem of the subsystem based off (5.9) and expressed in negative null form:

$$\text{min.} \quad -f(\boldsymbol{x},\boldsymbol{p}) = \frac{-24bc\rho\mathcal{M}_x - 32c^2b^4\rho^2 g_0\alpha + 3(m_b+m_p)^2 g_0\alpha}{24(m_b+m_p)g_0\alpha bc\rho} \tag{5.10}$$

$$\text{where} \quad \boldsymbol{x} = \left(\mathcal{M}_x, b, c, \alpha, m_b, m_p\right) \qquad x \in \mathbb{R}$$

$$\boldsymbol{p} = (\rho, g_0)$$

$$\text{s.t.} \quad h_1(\rho):\ \rho - 1000 = 0$$

$$h_2(g_0):\ g_0 - 9.81 = 0$$

$$g_1(\mathcal{M}_x, \alpha):\ \alpha\mathcal{M}_x \leq 0$$

$$g_2(m_p):\ m_p - 79 \leq 0$$

$$g_3(m_p):\ 53.3 - m_p \leq 0$$

$$g_4(m_b):\ 7.9 - m_b \leq 0$$

$$g_5(c):\ 0.9 - c \leq 0$$

$$g_6(c):\ c - 2.9 \leq 0$$

$$g_7(b):\ 0.15 - b \leq 0$$

$$g_8(b):\ b - 0.6 \leq 0$$

### 1) *Constraints and Parameters*

A set of constraints was applied to the analysed variables. These were derived from different principles, such as system characteristics, paddler anthropometrics and benchmarking against existing products. These constraints were annotated in the following table:

TABLE XVIII. SUBSYSTEM CONSTRAINT ANALYSIS

| Constraint | Description | Source |
|---|---|---|
| $g_1(\mathcal{M}_x, \alpha)$ | By definition, the restoring moment of the system counteracts the roll of the boat, hence is always of opposite sign to the tilt angle. | [31] |
| $g_2, g_3(m_p)$ | Taken from anthropometric studies of kayak paddlers, which show that their body masses usually range between 53.3 and 79 kg. | [32] |
| $g_4(m_b)$ | By benchmarking, the lightest kayaks available on the market start from 7.9 kg. | [33] |
| $g_5, g_6(c)$ | By benchmarking, the lengths of available kayaks (2c) range between 1.8 and 5.8 m. | [33] |
| $g_7, g_8(b)$ | By benchmarking, the widths of kayaks (2b) on the market range between 0.3 and 1.2 m. | [33] |

Similarly for system parameters:

TABLE XIX. SUBSYSTEM PARAMETER ANALYSIS

| Parameter | Description | Source |
|---|---|---|
| $h_1(\rho)$ | As stated in section I.B.1, the overall system is optimised for freshwater conditions with water density equal to 1000 kg/m$^3$. | |
| $h_2(g_0)$ | According to the International System of Units (SI), the conventional value of acceleration due to gravity is $980.665\,cm/s^2 \approx 9.81\,m/s^2$ | [34] |

### 2) *Assumptions and simplifications*

This subsystem optimization problem assumes that the kayak in question is being used at stable freshwater conditions, with all tilting caused by paddling and body movements, rather than waves or currents. The model kayaker's physique has been based on data on Olympic paddlers, assuming that people using kayaks for the purpose of fishing are of similar build. Furthermore, this subsystem neglects any effects the motor could have on the stability of the boat, by following the assumption that the kayak would be operated by either the paddle or the motor, but never by the two simultaneously – as seating height is said to raise paddling efficiency, it would not affect the speed of the boat while it is being powered by a motor. Finally, it is assumed that the only roll taking place is around the x-axis and that the symmetrical design of the kayak provides stability around y- and z-axes.

The subsystem has been simplified in order to make the understanding of the problem more straightforward. The shapes of the boat and the person operating it have been assumed to be two blocks with rectangular cross-sections (Fig. 14). As the positionings of the centers of gravity and buoyancy are derived geometrically, it would have required a lot of computational power to find their exact positionings on a human body and complex kayak shape. This simplification doesn't affect the logic behind the subsystem modelling.

## C. *Problem Space Exploration*

### 1) *Monotonicity Analysis*

A monotonicity analysis was conducted on the objective function in order to make sure that the problem is well bounded and to further simplify it where possible. Inactive constraints were identified, and will be disregarded in later steps of the problem.

TABLE XX. MONOTONICITY ANALYSIS

| Function | Variables | | | | | | Active? |
|---|---|---|---|---|---|---|---|
| | $\mathcal{M}_x$ | $b$ | $c$ | $\alpha$ | $m_p$ | $m_b$ | |
| $f$ | − | − | − | − | + | + | |
| $g_1(\mathcal{M}_x, \alpha)$ | + | | | − | | | *Yes* |
| $g_2(m_p)$ | | | | | + | | *No* |
| $g_3(m_p)$ | | | | | − | | *Yes* |
| $g_4(m_b)$ | | | | | | − | *Yes* |
| $g_5(c)$ | | | − | | | | *No* |
| $g_6(c)$ | | | + | | | | *Yes* |
| $g_7(b)$ | | − | | | | | *No* |
| $g_8(b)$ | | + | | | | | *Yes* |

### D. *Optimisation*

For the computational optimisation of the problem, two MatLab algorithms were used – fmincon and Sequential Quadratic Programming algorithm. These were later evaluated using Global Search to make sure that the values obtained in the calculations were not just local minima. The problem was constrained by active constraints identified in the previously conducted monotonicity analysis (Table 3), making it further simplified.

The following values for each of the variables were found by the previously mentioned algorithms:

TABLE XXI. OPTIMAL VARIABLE VALUES

| Algorithm | Optimal Value | | | | | |
|---|---|---|---|---|---|---|
| | $\mathcal{M}_x$ | $b$ | $c$ | $\alpha$ | $m_p$ | $m_b$ |
| ***fmincon*** | 0.0001 | 0.6 | 2.9 | -1.9996 | 7.9 | 53.3 |
| ***SQP*** | 9.8619e-05 | 0.6 | 2.9 | -1.9996 | 7.9 | 53.3 |
| ***Global Search*** | 0.0002 | 0.6 | 2.9 | -1.5758 | 7.9 | 53.3 |

Both fmincon and SQP algorithms found the final minimal value of the negative null function (5.10) to be equal to:

$$z_G = -0.1364$$

When converted back to the maximisation problem, that gives the height of the center of gravity of the human-kayak system as 0.1364 m above the waterline, as the highest possible position before the boat becomes unstable.

### E. *Discussion and Evaluation*

Fmincon and SQP were used as the main tools in the optimisation of the problem defined in this subsection. Both provided overlapping results, which were further confirmed to have been accurate representations by the use of the Global Search algorithm.

Using the algorithms in combination with monotonicity analysis has proven that the objective function is mostly dependent on restoration moment and tilt angle, as all the other variables would reach the values of their boundaries.

The model applied in this project gives satisfactory results, however it could be developed more thoroughly in future developments. One of the next steps would be the further exploration of the distribution of mass within the human body, as well as kayakers' seating positions, in order to find more realistic representations of the center of gravity. Same goes for the boat shape – a more accurate modelling of the problem could affect the final results and give more interesting insights.

Other assumptions made at the start of this subsystem might have also compromised the final result. Adding the effects of water movements and waves on the boar could affect the findings, by subjecting the boat to more unstable conditions. Some further user data analysis could be conducted to find a better representation for the kayak fishermen demographic and adding the complexity of using a motor to propel the kayak could bring interesting insights to the problem.

Overall, the modelling described in this report gives a good starting point to looking into how the seat position can affect kayakers' paddling efficiency, and by effect the overall speed of the kayak.

## VI. System Level Optimisation

A simple analytical model was used to integrate the different subsystems.

The maximum velocity of the boat before optimisation was found to be 1.5 m/s for human power and 4.5 m/s for motorised power. Once optimised, the result was found to be 3.00 m/s for human power and 10 m/s for motorised power.

This represents a 100% increase in velocity under paddle power and 120% increase in velocity under motor power.

## VII. Conclusion

After having optimised each individual section, all the variable outputs were fed into the Hull subsystem optimisation study to obtain results for the system-level problem formulation. The variables and constraints applied on the overall system level, were the same as the ones discussed in subsystem 1. The variables considered were the length, width and depth of the kayak. On the constraint side, the following were taken into consideration: Froude ratio, x-axis inertia, z-axis inertia, cross-section length, volume, seating depth, rotational distance. For a more in-depth analysis of variables see sections II.B.2 and II.B.3 and for the negative null form formulation applied in the overall system optimisation see equation (2.19). The final output on the system level was the speed of a fishing kayak equal to 3.0 m/s for human-powered and 10.0 m/s for motor-powered scenarios.

## VIII. REFERENCES


[1] Ahmed YM, Yaakob OB, Rashid MFA, Elbatran AH. Determining Ship Resistance Using Computational Fluid Dynamics (CFD). 2015;7.

[2] Howland J. Using Computational Fluid Dynamics to Predict Drag on a Boat Hull. :29.

[3] Usna.edu. 2019 [cited 12 December 2019]. Available from: https://www.usna.edu/NAOE/_files/documents/Courses/EN400/02.07%20Chapter%207.pdf

[4] Browning AW. A mathematical model to simulate small boat behaviour. SIMULATION. 1991 May;56(5):329–36.

[5] Michael J. Determinants of kayak paddling performance [Internet]. Taylor & Francis. 2019 [cited 12 December 2019]. Available from: https://www.tandfonline.com/doi/full/10.1080/14763140902745019?scroll=top&needAccess=true

[6] 1 Schaal L. How to win. the kayak Olympics. Or how to design and produce an innovative flatwater kayak paddle - PDF Free Download [Internet]. 2019 [cited 12 December 2019].

[7] Macdermid P, Osborne A, Stannard S. Mechanical Work and Physiological Responses to Simulated Flat Water Slalom Kayaking. 2019.

[8] Gomes B, Ramos N, Conceição F, Sanders R, Vaz M, Vilas-Boas J. Paddling Force Profiles at Different Stroke Rates in Elite Sprint Kayaking. Journal of Applied Biomechanics. 2015;31(4):258-263.

[9] MacPherson, S. (2015). *Propeller 101*. [online] Vicprop.com. Available at: https://www.vicprop.com/propeller101.htm.

[10] Amazon.com. (2019). [online] Available at: https://www.amazon.com/Minn-Kota-Endura-Transom-Trolling/dp/B07P1R5YV7.

[11] Gillmer, T. and Johnson, B. (1990). *Introduction to Naval Architecture*.

[12] Hepperle, M. (2018). *Propeller Design*. [online] Mh-aerotools.de. Available at: https://www.mh-aerotools.de/airfoils/jp_propeller_design.htm.

[13] Techet, A. (2005). *2.016 Hydrodynamics*. [online] Web.mit.edu. Available at: http://web.mit.edu/2.016/www/handouts/2005Reading10.pdf.

[14] Flite Test. (2013). *Propeller Static & Dynamic Thrust Calculation*. [online] Available at: https://www.flitetest.com/articles/propeller-static-dynamic-thrust-calculation.

[15] Inc., J. (2011). *Power and Torque: Understanding the Relationship Between the Two, by EPI Inc.*. [online] Epi-eng.com. Available at: http://www.epi-eng.com/piston_engine_technology/power_and_torque.htm.

[16] Scott, J. (2001). *Number of propeller blades*. [online] Heliciel.com. Available at: https://www.heliciel.com/en/helice/helice-propulsion/nombre-pales-helice-propulsion.htm.

[17] Epps, B., Viquez, O. and Chryssostomidis, C. (2015). *A Method for Propeller Blade Optimization and Cavitation Inception Mitigation*. [online] Available at: https://www.researchgate.net/publication/275281661_A_Method_for_Propeller_Blade_Optimization_and_Cavitation_Inception_Mitigation.

[18] Benson, T. (n.d.). *General Thrust Equation*. [online] Grc.nasa.gov. Available at: https://www.grc.nasa.gov/WWW/k-12/VirtualAero/BottleRocket/airplane/thrsteq.html.

[19] Staples, G. (2014). *Propeller Static & Dynamic Thrust Calculation - Part 2 of 2 - How Did I Come Up With This Equation?*. [online] Electricrcaircraftguy.com. Available at: https://www.electricrcaircraftguy.com/2014/04/propeller-static-dynamic-thrust-equation-background.html.

[20] Heads Up Hobby. (2019). *How to Calculate Propeller Pitch Speed - Heads Up Hobby*. [online] Available at: https://www.headsuphobby.com/calculate-propeller-pitch-speed/.

[21] Grc.nasa.gov. (2019). *Propeller Thrust*. [online] Available at: https://www.grc.nasa.gov/WWW/K-12/airplane/propth.html.

[22] Staples, G. (2013). *Propeller Thrust Calc.xlsx*. [online] Google Docs. Available at: https://docs.google.com/file/d/0BwHItOaHOOvdMGFLM1BmeWZLWGc/edit.

[23] LearningRC. (2015). *Brushless Motor Kv Constant Explained • LearningRC*. [online] Available at: http://learningrc.com/motor-kv/.

[24] Delafin, P. (2016). *Effect of the number of blades and solidity on the performance of a vertical axis wind turbine*. [online] Iopscience.iop.org. Available at: https://iopscience.iop.org/article/10.1088/1742-6596/753/2/022033/pdf.

[25] Precisionmicrodrives.com. (2019). *DC Motor Speed: Voltage and Torque Relationships - Precision Microdrives*. [online] Available at: https://www.precisionmicrodrives.com/content/dc-motor-speed-voltage-and-torque-relationships/.

[26] Vessels, N. (2019). *Trolling Motor*. [online] Newport Vessels. Available at: https://newportvessels.com/86lb-thrust-nv-series-saltwater-trolling-motor/.

[27] LaValley, E. (2002). *Density of Seawater - The Physics Factbook*. [online] Hypertextbook.com. Available at: https://hypertextbook.com/facts/2002/EdwardLaValley.shtml.

[28] Mecaflux.com. (n.d.). *HYDRODYNAMICS DRAG AND FLUID RESISTANCE*. [online] Available at: https://www.mecaflux.com/en/hydrodynamique.htm.

[29] Ong K, Elliott B, Ackland T, Lyttle A. Performance tolerance and boat set-up in elite sprint Kayaking. Sports Biomechanics. 2006;5(1):77-94.

[30] Broomfield S, Lauder M. Improving paddling efficiency through raising sitting height in female white water kayakers. Journal of Sports Sciences. 2015;33(14):1440-1446.

[31] Lautrup B. Physics of continuous matter. Boca Raton: Taylor & Francis; 2011.

[32] Ridge B, Broad E, Kerr D, Ackland T. Morphological characteristics of Olympic slalom canoe and kayak paddlers. European Journal of Sport Science. 2007;7(2):107-113.

[33] Length, Beam, Depth [Internet]. Cronus.rockisland.com. 2019 [cited 12 December 2019].

Available from: http://cronus.rockisland.com/~kyak/lbd.html

[34] The International System of Units (SI) [Internet]. Bipm.org. 2006 [cited 12 December 2019]. Available from: https://www.bipm.org/utils/common/pdf/si_brochure_8_en.pdf#page=51

# IX. APPENDICES

***NB - A digital appendix is available.***

## *A. Nomenclature*

| Symbol | Description | Units |
|---|---|---|
| $\boldsymbol{\rho}$ | Density | kg/m$^3$ |
| $\mathbf{V_s}$ | Velocity of boat | |
| $\mathbf{V_s}\boldsymbol{Max}$ | Maximum velocity of boat | |
| $\mathbf{F_{paddle}}$ | Force outputted by the paddle | |
| $\mathbf{F}_{\boldsymbol{motor}}$ | Force outputted by the paddle | |
| $\mathbf{R_t}$ | Hull resistance of linear travel | |
| $\mathbf{R}_{\boldsymbol{rot}}$ | Hull resistance of rotational travel | |
| **L** | Length | |
| **B** | Maximum width of Hull | |
| **D** | Maximum depth of Hull | |
| **T** | Wetted depth of Hull | |
| | | |
| **d** | Propeller diameter | inches |
| **p** | Pitch | inches |
| **b** | Blade number | |
| **c** | Chord length | inches |
| **v** | voltage | volts |
| $\mathbf{K_v}$ | Motor velocity constant | |
| m | Mass | kg |
| **ΔV** | Change in velocity | m/s |
| $\mathbf{V_e}$ | Velocity of exit | m/s |
| $\mathbf{V_f}$ | Freestream velocity | m/s |
| $\mathbf{m_{dot}}$ | Mass flow rate | Kg/m |
| A | Cross sectional area | m$^2$ |
| $\mathbf{V_p}$ | Pitch speed | m/s |
| RPM | Revolutions per minute | rpm |
| $\mathcal{M}_x$ | Restoration moment | |
| $\alpha$ | Tilt angle | |
| $z_B$ | Center of buoyancy in z-axis | m |
| $z_G$ | Center of gravity in z-axis | m |
| $I_0$ | Second moment of inertia | |
| $V_0$ | Displaced volume of water | $m^3$ |
| M | Total mass of human-kayak system | kg |
| $g_0$ | Gravitational acceleration | $m/s^2$ |

## *A. Benchmark Boat*

| Variable | Value |
|---|---|
| Length | $\boldsymbol{3.08\,m}$ |
| Width | $\boldsymbol{0.750\,m}$ |
| Depth | $\boldsymbol{0.350\,m}$ |
| Velocity | $\boldsymbol{1.55\,m/s}$ |
| Rotational velocity | $\boldsymbol{0.1542\,rads^{-1}}$ |

## *B. Subsystem 2*

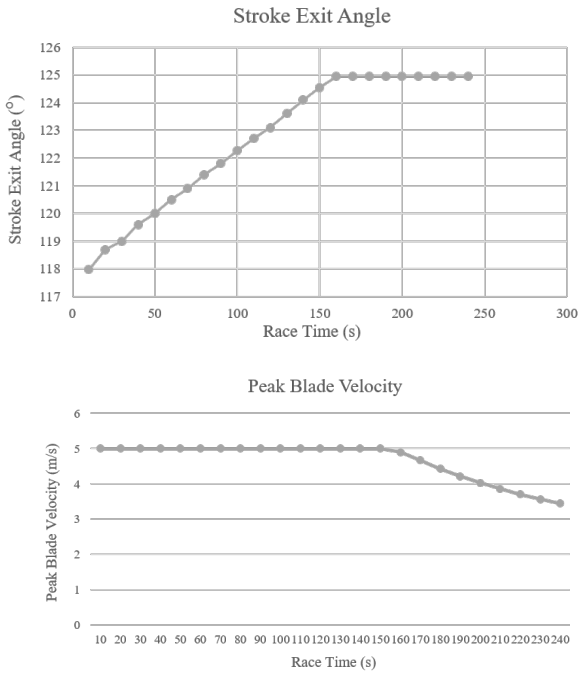


**Figure 1**